

Provided for non-commercial research and education use.  
Not for reproduction, distribution or commercial use.



This article appeared in a journal published by Elsevier. The attached copy is furnished to the author for internal non-commercial research and education use, including for instruction at the authors institution and sharing with colleagues.

Other uses, including reproduction and distribution, or selling or licensing copies, or posting to personal, institutional or third party websites are prohibited.

In most cases authors are permitted to post their version of the article (e.g. in Word or Tex form) to their personal website or institutional repository. Authors requiring further information regarding Elsevier's archiving and manuscript policies are encouraged to visit:

<http://www.elsevier.com/copyright>



## Notices to investigation of symbiotic binaries IV. Optical light curves from the near-ultraviolet

A. Skopal

Astronomical Institute, Slovak Academy of Sciences, 059 60 Tatranská Lomnica, Slovakia

### ARTICLE INFO

#### Article history:

Received 14 May 2008

Received in revised form 22 August 2008

Accepted 5 October 2008

Available online 17 October 2008

Communicated by E.P.J. van den Heuvel

#### PACS:

97.30.Eh

97.30.Qt

97.80.Gm

#### Keywords:

Techniques: photometric

Stars: binaries

Symbiotics

### ABSTRACT

The aim of this note is to reconstruct optical light curves (LC) from the near-UV fluxes of the ultraviolet spectra of symbiotic binaries during their quiescent phases. The method is based on the fact that the nebular component of radiation dominates the near-UV during quiescent phases and represents the main source of the light variability in the optical. We demonstrate this approach on example of two quiet symbiotic stars, SY Mus and RW Hya. Using their *IUE* spectra we determined *U* and *B* magnitudes in the standard Johnson system. Values derived from the near-ultraviolet are fainter than those measured photometrically by  $\Delta U \approx 0.2$  and  $\Delta B \approx 0.4$ . This difference is due to emission lines.

© 2008 Elsevier B.V. All rights reserved.

### 1. Introduction

Symbiotic stars are long-period ( $P_{\text{orb}} \sim 1 - 3$  years or more) interacting binary systems consisting of a late-type giant and a hot compact star, believed to be a white dwarf. During the so-called *quiescent* phases the white dwarf accretes a fraction of the wind from the giant, which heats up its surface to a very high temperature of  $T_{\text{h}} \sim 10^5$  K, enhances its luminosity to  $L_{\text{h}} \sim 10^2 - 10^4 L_{\odot}$  and enlarges its effective radius to  $\sim 0.1 R_{\odot}$  in the ultraviolet (cf. Table 3 and Fig. 26 in Skopal, 2005). Such a hot and luminous source of radiation then ionizes the winds from both the stars in the binary, giving rise to nebular emission. As a result, the observed spectrum of symbiotic stars is composed of three basic components of radiation – two stellar,  $F_{\text{H}}(\lambda)$  and  $F_{\text{G}}(\lambda)$ , from the hot star and the cool giant, respectively, and one nebular,  $F_{\text{N}}(\lambda)$ , dominated by the component from the ionized fraction of the giant's wind. Thus the observed flux in the continuum,  $F(\lambda)$ , is given by superposition of all these contributions, i.e.

$$F(\lambda) = F_{\text{G}}(\lambda) + F_{\text{H}}(\lambda) + F_{\text{N}}(\lambda). \quad (1)$$

Throughout the optical they rival each other, producing a composite spectrum that is often characterized with bizarre colour indices. In

addition, the three components can be very different for individual objects, and are subject to variation according to the orbital phase of the binary and/or its activity.

Generally, during quiescent phases the nebular flux usually dominates the near-UV and optical *U* spectral region, whereas at longer wavelength, from about *B* band, the observed flux is dominated by that from the giant (cf. model SEDs in Skopal, 2005). In addition, the symbiotic nebula is partially optically thick, which causes its apparent variation as a function of the orbital phase. This orbitally-related wave-like variation is characterized with a sinusoidal profile of the LC along the orbit, whose minima and maxima occur around the inferior and superior conjunction of the giant, respectively. The magnitude difference between the minimum and maximum,  $\Delta m \sim 1 - 2$  mag, and, in agreement with the flux distribution of individual components of radiation (Eq. (1)), is always larger in the blue part of the spectrum than in the red one. For example, in the *UBV* photometric system,  $\Delta U > \Delta B > \Delta V$ . This type of variability was originally interpreted in terms of a reflection effect, in which the hot star irradiates the facing giant's hemisphere (e.g. Belyakina, 1970). Skopal (2001a) investigated this wave-like modulation within the simple ionization model as proposed by Seaquist et al. (1984). He found that the model emission measure (EM) is equivalent to the observed one, and that its variation produces that observed in LCs. Recently, Skopal (2007b)

E-mail address: [skopal@ta3.sk](mailto:skopal@ta3.sk)

demonstrated the connection between the amount of EM and stellar  $B$ -magnitude for V1329 Cyg by modeling the optical SED at different orbital positions of the binary.

In this paper, we describe the method to reconstruct the LCs of quiescent symbiotic stars from their ultraviolet spectra (Section 2). In Section 3, we apply it to two quiet symbiotic stars, SY Mus and RW Hya with the main aim to enrich their scanty photometric measurements. In Section 4, we compare both the reconstructed and the measured magnitudes, and discuss the results.

Finally, we note that this contribution follows previous notices to investigation of symbiotic stars (Skopal, 2000, 2001b; Csátryová and Skopal, 2005), which are aimed to point out some interesting properties of symbiotic stars that can be useful in their investigation.

## 2. The method

The stellar magnitude given by the *nebular* component of radiation in the spectrum of a symbiotic star, measured through a photometric filter characterized with the effective wavelength  $f$ , can be expressed as (Skopal, 2001a, Eq. (14))

$$m_N(f) = -2.5 \log(EM) + C_f, \quad (2)$$

where  $C_f = q_f - 2.5 \log(\varepsilon_f/4\pi d^2)$ ,  $q_f$  defines the zero of the magnitude scale at the given passband,  $\varepsilon_f$  is the volume emission coefficient per electron and ion at the wavelength  $f$  of the considered filter and  $d$  is the distance to the object. For the standard Johnson  $UBV$  photometric system and fluxes in units of  $\text{erg cm}^{-2}\text{s}^{-1}\text{\AA}^{-1}$ ,  $q_U = -20.9$ ,  $q_B = -20.36$  and  $q_V = -21.02$  (e.g. Henden and Kaitchuck, 1982). The quantity of  $EM$  is determined by the volume of the ionized zone  $V$  and concentrations of ions,  $n_+$ , and electrons,  $n_e$  as

$$EM = \int_V n_+ n_e dV = 4\pi d^2 \frac{F_N(\lambda)}{\varepsilon_\lambda}, \quad (3)$$

where  $F_N(\lambda)$  is the measured flux of the nebular continuum and  $\varepsilon_\lambda$  is the volume emission coefficient at the wavelength  $\lambda$ . Accordingly, Eq. (2) can be written in the form

$$m_N(f) = -2.5 \log\left(\frac{\varepsilon_f}{\varepsilon_\lambda} F_N(\lambda)\right) + q_f, \quad (4)$$

where the ratio  $\varepsilon_f/\varepsilon_\lambda$  scales the nebular flux  $F_N(\lambda)$  to that contributing at the wavelength  $f$  of a photometric filter. For practical use we plotted this ratio in Fig. 1 for  $U$  and  $B$  filters, and three selected electron temperatures ( $T_e$ ). Eq. (4) can be used to determine the stellar magnitude only in the passbands, in which the nebular emission dominates the spectrum. However, radiation of symbiotic stars is composed of three basic components (Eq. (1)). Therefore, to derive optical magnitudes, contributions from other sources have to be in-

cluded. According to model SEDs the nebular component of radiation usually dominates the near-UV/U spectral region during quiescent phases and the outbursts of the second type (Skopal, 2005). In these cases, light contribution from the hot star can be neglected in the optical, because of its very high temperature ( $T_h \geq 10^5\text{K}$ ). However, radiation from the giant has to be considered. Then, Eq. (4) can be written in a more general form as

$$m(f) = -2.5 \log\left(\frac{\varepsilon_f}{\varepsilon_\lambda} F_N(\lambda) + F_G(f)\right) + q_f, \quad (5)$$

where  $F_G(f)$  is the flux from the giant at the effective wavelength of the filter,  $f$ . This quantity can be taken directly from available SEDs of giants in symbiotic stars (e.g. Skopal, 2005) or estimated from their spectral type (e.g. Mürset and Schmid, 1999), corresponding colour indices or synthetic models (Lee, 1970; Kučinskas et al., 2005) scaled to an IR magnitude. From the  $B$  band to longer wavelengths the  $F_G(f)$  flux must be included, otherwise the magnitudes inferred from Eq. (5) will be fainter. Also the phase-independent contribution from the giant produces a lower amplitude of the orbitally-related variation caused by the nebula. Finally, we note that Eq. (5) cannot be used for systems during the 1st-type of outbursts, because a warm shell of the *stellar* nature dominates the optical (cf. Fig. 26 of Skopal, 2005).

To determine magnitudes according to Eq. (5) one needs to estimate and *deredden* the nebular flux-point at an appropriate wavelength of the UV continuum (we suggest the region between 3000 and 3200 Å for *IUE* spectra). Then to transform this flux to the effective wavelength of the considered filter by multiplying it with the factor of  $\varepsilon_f/\varepsilon_\lambda$  (Fig. 1), to add relevant constants,  $F_G(f)$  and  $q_f$ , and to *redde*n these magnitudes to be comparable with the observed photometric measurements. Note that it would be incorrect to derive magnitudes directly from the *observed* UV fluxes, because the extinction curve is a wavelength-dependent function. It is important to take into account that the magnitudes given by Eq. (5) correspond to those of the net continuum. They do not include the effect of emission lines and therefore are fainter than those obtained directly by the standard photometry (see Skopal, 2007a in detail).

Finally, we calculated the volume emission coefficient for hydrogen plasma only including contributions from recombination and bremsstrahlung as introduced by Skopal (2001b). According to the asymmetry of the  $U$  filter with respect to the wavelength of the Balmer discontinuity,  $\lambda_B$ , we calculated the emission coefficient  $\varepsilon_U$  as the weighted average of its values from both the sides of the Balmer jump as

$$\varepsilon_U = \frac{[\varepsilon_- \int_0^{\lambda_B} S_\lambda d\lambda + \varepsilon_+ \int_{\lambda_B}^\infty S_\lambda d\lambda]}{\int_0^\infty S_\lambda d\lambda}, \quad (6)$$

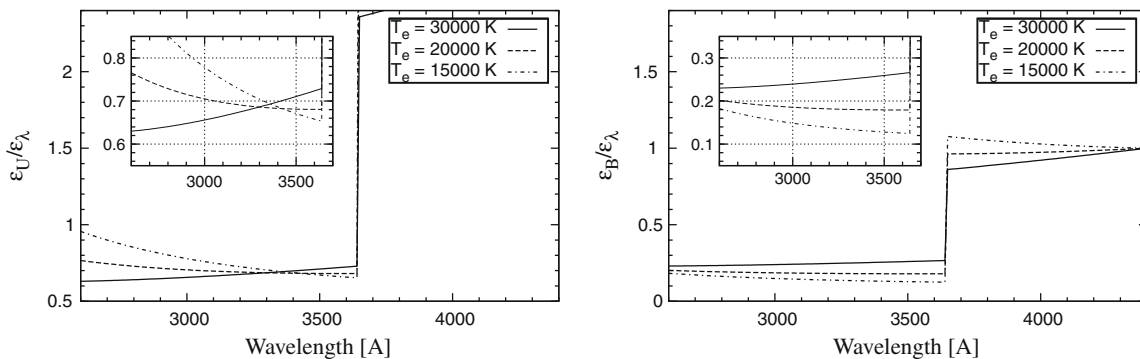


**Fig. 1.** The ratios  $\varepsilon_U/\varepsilon_\lambda$  and  $\varepsilon_B/\varepsilon_\lambda$  for  $T_e = 15,000, 20,000$  and  $30,000$  K. According to Eq. (5), the nebular flux at, for example,  $\lambda 3100\text{\AA}$  is converted to the  $U(f = 3650\text{\AA})$  and  $B(f = 4400\text{\AA})$  bands by multiplication with a factor of  $\sim 0.7$  and  $\sim 0.2$ , respectively.

where  $S_\lambda$  is the response function for the  $U$  filter, and  $\varepsilon_-$  and  $\varepsilon_+$  are coefficients at the short and long wavelength side of  $\lambda_B$ , respectively. For the sake of simplicity, we assumed them to be constant within the filter width. For the  $U$  response function defined by, for example, Matthews and Sandage (1963) or Johnson (1965),  $\varepsilon_U = (1.17 - 1.11) \times 0.5(\varepsilon_- + \varepsilon_+)$  for  $T_e = 15,000 - 35,000\text{K}$ .

### 3. Example objects

We demonstrate this method for symbiotic stars during quiescent phases, whose radiation throughout the near-UV spectrum is dominated by the nebular emission (Section 1). In addition, we selected objects with a high orbital inclination, where a large amplitude of the wave-like orbitally-related variations can be expected. As a result, for the purpose of this paper, we reconstruct the  $U$  and  $B$  LCs for two quiet eclipsing symbiotic stars, RW Hya and SY Mus, with the main aim to enrich their scanty multicolour photometric measurements. In both cases we use calibrated ultraviolet spectra from the archive of the *IUE* satellite. The results are summarized in Table 2 and plotted in Fig. 2.

#### 3.1. RW Hya

RW Hya is a classical symbiotic binary harbouring a white dwarf accreting material from a cool M2 III giant (Mürset and Schmid, 1999) on a 370.4-day orbit (Schild et al., 1996). RW Hya is a stable symbiotic system – no optical eruption of the Z And-type has been observed to date. Its LC displays a wave-like variation as a function of the orbital phase (Fig. 2). However, its  $UBV$  photometric measurements are very scanty. Only a few observations were published by Munari et al. (1992) and Skopal et al. (2004). In addition, its orbital period of roughly 1 year makes it difficult to cover the whole phased LC by the ground-based observations. The system of RW Hya has a high inclination of the orbital plane as indicated by the eclipse effect due to attenuation of the far-UV continuum by Rayleigh scattering on atomic hydrogen (e.g. Schild et al., 1996). Therefore, one can expect a pronounced variations in the  $U$  passband, where the contribution from the nebula is dominant (see Fig. 17 in Skopal, 2005).

For the purpose of this paper we selected all available *IUE* spectra made by the long wavelength prime and taken through the

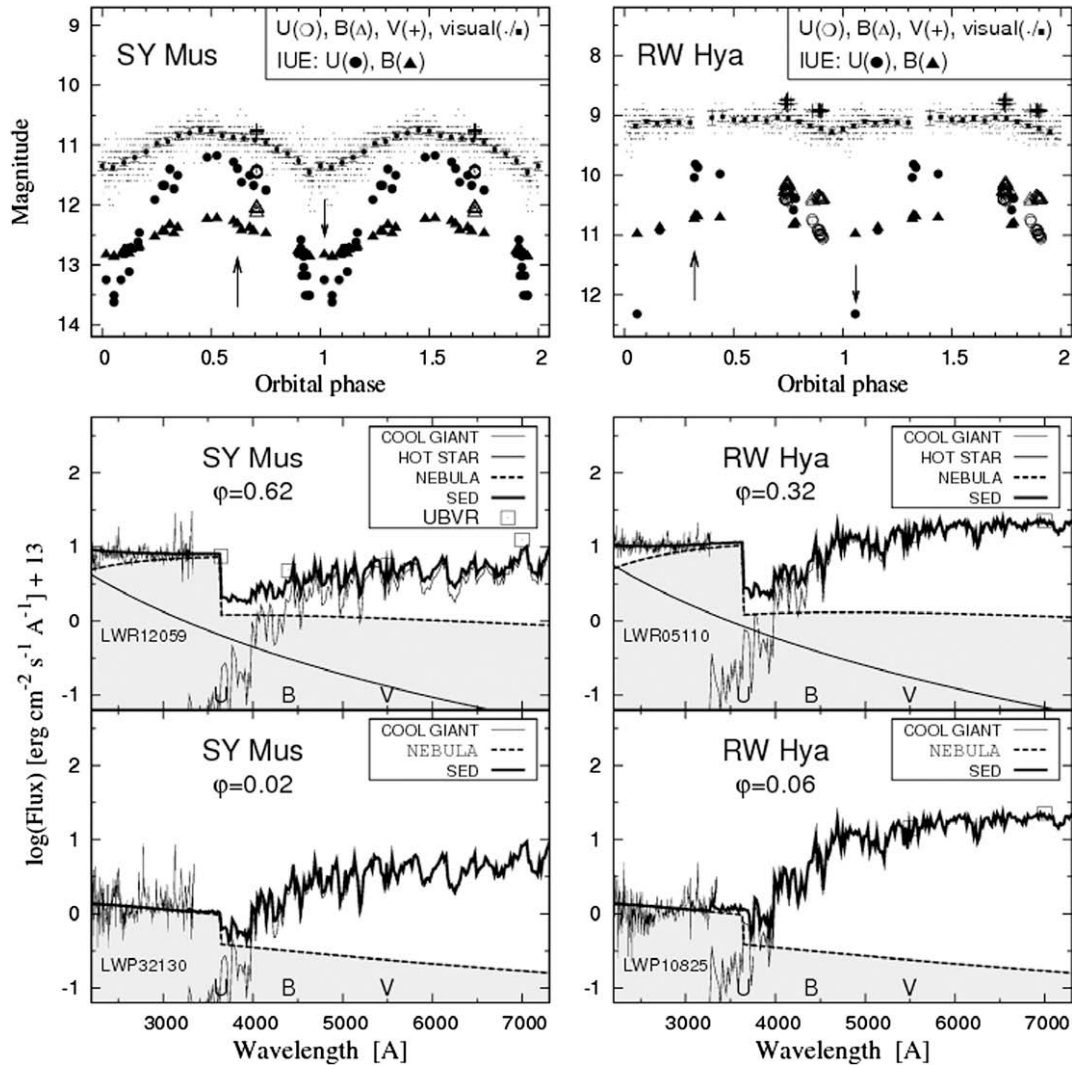


**Fig. 2.** LCs and SEDs for SY Mus and RW Hya. Top panels show  $UBV$  and visual LCs as a function of the orbital phase. Values derived from the *IUE* spectra (full symbols,  $U_{\text{obs}}$  and  $B_{\text{obs}}$  in Tables 1 and 2) are fainter than those measured directly by means of stellar photometry (open symbols), due to the effect of emission lines (see the text). Bottom panels show the optical SEDs with isolated main components of radiation from the giant, hot star and nebula. The SEDs were reconstructed according to Skopal (2005) around times of spectroscopic conjunctions of the binary components (marked by arrows in top panels) to demonstrate also the nature of the orbitally-related modulation, which is due to apparent variation in the nebular flux (shaded region).

large aperture. We measured fluxes at  $\lambda 3200 \text{ \AA}$  and converted them to  $U$  and  $B$  magnitudes according to Eq. (5) by using the ratios  $\epsilon_U/\epsilon_{3200} = 0.72$  and  $\epsilon_B/\epsilon_{3200} = 0.14$  that correspond to  $T_e = 15000\text{K}$  (Fig. 1). The contribution from the giant into the  $B$  pass-band was estimated to  $F_G(B) \sim 4.0 \times 10^{-13} \text{ erg cm}^{-2} \text{ s}^{-1} \text{ \AA}^{-1}$  (Fig. 2). The distance to RW Hya,  $d = 820\text{pc}$  (Skopal, 2005) and the coefficient  $\epsilon_{3200} = 3.4 \times 10^{-28} \text{ erg cm}^{-3} \text{ s}^{-1} \text{ \AA}^{-1}$  were used to determine the emission measure according to Eq. (3). Measured fluxes were dereddened with  $E_{B-V} = 0.1$  (Mürset et al., 1991).

### 3.2. SY Mus

SY Mus is another stable symbiotic star, in which a white dwarf accretes material from a cool M4.5 III giant (Mürset and Schmid, 1999) on a 625-day orbit (e.g. Dumm et al., 1999). The system is eclipsing, the Rayleigh scattering significantly attenuates the far-

UV continuum around Ly- $\alpha$  when the binary approaches the position of the inferior giant's conjunction and the light from the hot star disappears entirely from the spectrum (e.g. Pereira et al., 1995). The visual LC of SY Mus displays a strictly periodic orbital-related wave-like variation (Fig. 2). Due to its location on the southern sky, SY Mus was rarely observed from the ground-based observatories (Schmutz et al., 1994). As a result its multicolour optical photometry is very scanty (Skopal et al., 2007). However, SY Mus had been observed intensively by the *IUE* satellite during its whole lifetime. Strong variations in the UV flux were studied by more authors (e.g. Schmutz et al., 1994, 1995, 1999). A variation in the emission measure along the orbital phase was pointed out by Skopal (2005). Therefore, SY Mus is a desirable system to enrich its optical photometry by our method.

To reconstruct LCs from the ultraviolet spectroscopy we measured continuum fluxes at  $\lambda 3100 \text{ \AA}$  on all available LWP[R] *IUE*

**Table 1**

$U$  and  $B$  magnitudes derived from *IUE* spectra of RW Hya. Indices 'der' and 'obs' denote dereddened and observed quantity, respectively.  $U_{\text{obs}}$  and  $B_{\text{obs}}$  values are plotted in Fig. 2.

Spectrum	Date	JD 2 4 . .	Phase <sup>a</sup>	$F_{\text{der}}(3200)$ (erg cm <sup>-2</sup> s <sup>-1</sup> Å <sup>-1</sup> )	$EM(\text{cm}^{-3})$	$U_{\text{der}}$ (mag)	$U_{\text{obs}}$ (mag)	$B_{\text{der}}$ (mag)	$B_{\text{obs}}$ (mag)
LWR03358	January 02, 79	43875.79	0.784	6.5E-13	1.5E+59	9.92	10.39	10.41	10.80
LWR05110	July 19, 79	44074.25	0.319	9.0E-13	2.1E+59	9.57	10.04	10.34	10.73
LWR05139	July 21, 79	44076.28	0.324	11.0E-13	2.6E+59	9.35	9.82	10.28	10.67
LWR05167	July 25, 79	44080.24	0.335	10.5E-13	2.5E+59	9.40	9.87	10.30	10.69
LWR05481	September 01, 79	44117.84	0.437	9.5E-13	2.3E+59	9.51	9.98	10.32	10.71
LWR09667	January 08, 81	44613.21	0.774	5.5E-13	1.3E+59	10.11	10.58	10.44	10.83
LWP06252	June 21, 85	46238.17	0.161	4.0E-13	9.5E+58	10.45	10.92	10.49	10.88
LWP10825	May 24, 87	46940.37	0.057	1.1E-13	2.6E+58	11.85	12.32	10.59	10.98

<sup>a</sup>  $JD_{\text{sp. conj.}} = 2,449,512 + 370.4 \times E$  Schild et al. (1996).

**Table 2**

As in Table 1, but for SY Mus.

Spectrum	Date	JD 2 4 . .	Phase <sup>a</sup>	$F_{\text{der}}(3100)$ (erg cm <sup>-2</sup> s <sup>-1</sup> Å <sup>-1</sup> )	$EM(\text{cm}^{-3})$	$U_{\text{der}}$ (mag)	$U_{\text{obs}}$ (mag)	$B_{\text{der}}$ (mag)	$B_{\text{obs}}$ (mag)
LWR08855	September 21, 80	44503.6	0.924	2.0E-13	8.7E+58	11.23	12.86	11.42	12.77
LWR10828	June 11, 81	44766.9	0.346	7.0E-13	3.0E+59	9.87	11.50	11.03	12.38
LWR12059	November 29, 81	44938.5	0.620	7.8E-13	3.4E+59	9.76	11.39	10.97	12.32
LWR12116	December 11, 81	44949.6	0.639	6.3E-13	2.7E+59	9.99	11.62	11.07	12.42
LWR01263	February 19, 82	45020.3	0.751	5.6E-13	2.4E+59	10.12	11.75	11.12	12.47
LWP03354	May 13, 84	45834.2	0.054	1.1E-13	4.8E+58	11.88	13.51	11.51	12.86
LWP15824	July 2, 89	47709.6	0.054	1.0E-13	4.4E+58	11.99	13.62	11.52	12.87
LWP16306	September 8, 89	47778.2	0.164	2.5E-13	1.1E+59	10.99	12.62	11.37	12.72
LWP16966	December 20, 89	47881.1	0.329	5.7E-13	2.5E+59	10.10	11.73	11.12	12.47
LWP17598	March 25, 90	47975.9	0.481	9.3E-13	4.0E+59	9.57	11.20	10.88	12.23
LWP18063	June 9, 90	48051.7	0.602	8.6E-13	3.7E+59	9.65	11.28	10.92	12.27
LWP18527	August 5, 90	48109.1	0.694	6.0E-13	2.6E+59	10.04	11.67	11.09	12.44
LWP19567	January 13, 91	48270.0	0.951	1.1E-13	4.8E+58	11.88	13.51	11.51	12.86
LWP20180	April 18, 91	48364.8	0.103	2.1E-13	9.1E+58	11.18	12.81	11.41	12.76
LWP20798	July 13, 91	48450.6	0.241	4.8E-13	2.1E+59	10.28	11.91	11.18	12.53
LWP20951	August 4, 91	48473.4	0.276	6.0E-13	2.6E+59	10.04	11.67	11.09	12.44
LWP20982	August 10, 91	48478.5	0.286	6.0E-13	2.6E+59	10.04	11.67	11.09	12.44
LWP21082	August 25, 91	48494.5	0.310	7.7E-13	3.4E+59	9.77	11.40	10.98	12.33
LWP22205	January 7, 92	48628.9	0.526	9.5E-13	4.1E+59	9.54	11.17	10.87	12.22
LWP22777	April 10, 92	48722.6	0.676	7.0E-13	3.0E+59	9.87	11.50	11.03	12.38
LWP23798	August 29, 92	48863.5	0.902	2.1E-13	9.1E+58	11.18	12.81	11.41	12.76
LWP28131	May 15, 94	49487.6	0.898	2.1E-13	9.1E+58	11.18	12.81	11.41	12.76
LWP28266	May 26, 94	49498.5	0.916	1.5E-13	6.5E+58	11.55	13.18	11.47	12.82
LWP28324	June 4, 94	49508.4	0.932	1.1E-13	4.8E+58	11.88	13.51	11.51	12.86
LWP28422	June 15, 94	49518.5	0.948	1.1E-13	4.8E+58	11.88	13.51	11.51	12.86
LWP31938	February 6, 96	50119.8	0.911	2.6E-13	1.1E+59	10.95	12.58	11.36	12.71
LWP31985	February 14, 96	50127.8	0.924	1.7E-13	7.4E+58	11.41	13.04	11.45	12.80
LWP32019	February 23, 96	50136.7	0.938	1.5E-13	6.5E+58	11.55	13.18	11.47	12.82
LWP32130	April 13, 96	50186.9	0.018	1.4E-13	6.1E+58	11.62	13.25	11.48	12.83
LWP32308	May 25, 96	50228.7	0.086	1.4E-13	6.1E+58	11.62	13.25	11.48	12.83
LWP32324	June 1, 96	50235.5	0.097	2.1E-13	9.1E+58	11.18	12.81	11.41	12.76
LWP32333	June 4, 96	50238.5	0.102	2.1E-13	9.1E+58	11.18	12.81	11.41	12.76
LWP32349	June 7, 96	50241.6	0.106	2.1E-13	9.1E+58	11.18	12.81	11.41	12.76
LWP32362	June 11, 96	50246.4	0.113	2.2E-13	9.6E+58	11.13	12.76	11.40	12.75
LWP32370	June 18, 96	50252.6	0.124	1.6E-13	7.0E+58	11.48	13.11	11.46	12.81
LWP32371	June 23, 96	50257.6	0.132	2.3E-13	1.0E+59	11.08	12.71	11.39	12.74
LWP32383	July 17, 96	50281.9	0.170	2.9E-13	1.3E+59	10.83	12.46	11.34	12.69

<sup>a</sup>  $JD_{\text{sp. conj.}} = 2,450,176 + 625 \times E$  Dumm et al. (1999).

spectra taken through the large aperture. According to the model SED ( $T_e = 18,500$  K, Skopal, 2005) we used the ratios  $\epsilon_U/\epsilon_{3100} = 0.70$  and  $\epsilon_B/\epsilon_{3100} = 0.17$  to convert the nebular flux from the ultraviolet to  $U$  and  $B$  magnitudes (Eq. (5), Fig. 1). The  $B$ -band flux from the giant was estimated to  $F_G(B) = 1.6 \times 10^{-13}$  erg cm $^{-2}$  s $^{-1}$  Å $^{-1}$  (Fig. 2). Observed fluxes were dereddened with  $E_{B-V} = 0.35$ , and to determine  $EM$  we used the distance to SY Mus of 1 kpc (Skopal, 2005) and the emission coefficient  $\epsilon_{3100} = 2.75 \times 10^{-28}$  erg cm $^{+3}$  s $^{-1}$  Å $^{-1}$ .

## 4. Discussion

### 4.1. The effect of emission lines

The optical magnitudes derived by our method correspond to the net continuum, while those measured photometrically include contributions from both the continuum and the lines. The effect of emission line spectrum of quiescent symbiotic stars on the measured  $U$  and  $B$  magnitudes is of a few  $\times 0.1$  mag (Skopal, 2007a). Therefore, the shift between the reconstructed and measured LCs of  $\Delta U \approx +0.2$  and  $\Delta B \approx +0.4$ , revealed for our cases of SY Mus and RW Hya (Fig. 2), can be ascribed to this effect. In addition, the effect of emission lines varies probably with the orbital phase. At the time of the inferior conjunction of the giant, it is larger due to the lower level of the continuum than at the opposite position (Skopal, 2007a). As a result the amplitude of the wave-like variation inferred from the UV continuum can be expected to be somewhat larger than that measured photometrically.

### 4.2. Wave-like variation and the SED

The variation in the  $U$  and  $B$  magnitudes obtained by our method is strictly periodic with the orbital phase, and is wave-like in the profile. This behaviour is consistent with conditions during quiescent phases of symbiotic stars. We briefly comment on their main characteristics as follows:

- (i) In both cases the LCs show  $\Delta U > \Delta B$ . This has an origin in apparent orbital changes of the nebular component of the radiation and in the fact that the contribution from the giant, which does not depend on the orbital phase, strengthens towards the longer wavelengths (Fig. 2, Eq. (5)).
- (ii) A large amplitude,  $\Delta U \sim 2.2$ mag, was revealed for both systems. This is due to the dominant contribution from the nebula within the  $U$  passband (Fig. 2,  $F_N(U) \gg F_G(U)$ ), and due to the fact that the  $EM$  and orbital inclination for both the systems are very similar (Tables 1 and 2).
- (iii) However,  $\Delta B(\text{SY Mus}) \sim 0.6 > \Delta B(\text{RW Hya}) \sim 0.3$ mag. This difference is caused by the earlier spectral type of the giant in RW Hya (M2,  $T_{\text{eff}} \sim 3800$ K) than in SY Mus (M4.5,  $T_{\text{eff}} \sim 3400$ K), because the ratio  $F_N(\lambda)/F_G(\lambda)$  decreases more rapidly with wavelength for earlier spectral type of the giant (Fig. 2).

### 4.3. Sources of uncertainties

The uncertainties of the magnitudes derived by our method are due to those of the UV continuum fluxes and  $T_e$ . The long-wave-

length part of the LWP[R] spectra were usually well exposed, having uncertainties of about 5%, which transforms into  $\Delta m \sim 0.05$ mag (cf. Eq. (4)). The possible uncertainty in  $T_e$  transforms to that of the scaling factor  $\epsilon_f/\epsilon_\lambda$ , which is a wavelength dependent function. At  $\lambda \sim 3350$  Å the factor  $\epsilon_U/\epsilon_\lambda$  practically does not depend on  $T_e$  (Fig. 1). However,  $\epsilon_B/\epsilon_\lambda = 0.14$ – $0.25$  at this wavelength for  $T_e = 15,000$ – $30,000$ K, producing a maximum range of uncertainties of  $\Delta B \sim 0.6$ mag.

## 5. Conclusion

We introduced a method on how to convert the near-UV fluxes of quiescent symbiotic binaries into the scale of the optical magnitudes (Section 2). The method is based on the fact that the nebular emission dominates the near-ultraviolet and represents the main source of the periodic variability in the optical light. We applied the method to symbiotic stars, RW Hya and SY Mus. Using their  $IUE$  spectra we determined corresponding  $U$  and  $B$  magnitudes of the Johnson system (Fig. 2). They enriched significantly current data-sets of photometric measurements for both the stars, mainly for SY Mus. The reconstructed magnitudes are fainter than directly measured quantities by  $\sim 0.2$  and  $\sim 0.4$ mag in  $U$  and  $B$ , respectively. This difference is caused by the effect of emission lines on the photometric magnitudes. By this way we also demonstrated the nature of the wave-like orbitally-related variation in the LCs of symbiotic stars as a result of the apparent periodic variation in the  $EM$  along the orbital phase.

## Acknowledgement

This research was supported by a grant of the Slovak Academy of Sciences No. 2/7010/27.

## References

- Belyakina, T.S., 1970. *Astrofizika* 6, 49.  
 Csatóryová, M., Skopal, A., 2005. *Contrib. Astron. Obs. Skalnaté Pleso* 35, 17.  
 Dumm, T., Schmutz, W., Schild, H., Nussbaumer, H., 1999. *A&A* 349, 169.  
 Henden, A.A., Kaitchuck, R.H., 1982. *Astronomical Photometry*. Van Nostrand Reinhold, Company, New York.  
 Johnson, H.L., 1965. *ApJ* 141, 923.  
 Kučinskas, A., Hauschildt, P.H., Ludwig, H.-G., Brott, I., Vansevičius, V., Lindegren, L., Tanabé, T., Allard, F., 2005. *A&A* 442, 281.  
 Lee, T.A., 1970. *ApJ* 162, 217.  
 Matthews, T.A., Sandage, A.R., 1963. *ApJ* 138, 30.  
 Munari, U., Yudin, B.F., Taranova, O.G., et al., 1992. *A&ASS* 93, 383.  
 Mürset, U., Schmid, H.M., 1999. *A&AS* 137, 473.  
 Mürset, U., Nussbaumer, H., Schmid, H.M., Vogel, M., 1991. *A&A* 248, 458.  
 Pereira, C.B., Vogel, M., Nussbaumer, H., 1995. *A&A* 293, 783.  
 Schild, H., Mürset, U., Schmutz, W., 1996. *A&A* 306, 477.  
 Schmutz, W., Schild, H., Mürset, U., Schmid, H.M., 1994. *A&A* 288, 819.  
 Seaquist, E.R., Taylor, A.R., Button, S., 1984. *ApJ* 284, 202.  
 Skopal, A., 2000. *Contrib. Astron. Obs. Skalnaté Pleso* 30, 21.  
 Skopal, A., 2001a. *A&A* 366, 157.  
 Skopal, A., 2001b. *Contrib. Astron. Obs. Skalnaté Pleso* 31, 119.  
 Skopal, A., 2005. *A&A* 440, 995.  
 Skopal, A., 2007a. *New. Astron.* 12, 597.  
 Skopal, A., 2007b. *J. Amer. Assoc. Var. Star Obs.* 36 preprint no. 65, [arxiv:0805.1222].  
 Skopal, A., Pribulla, T., Vaňko, M., et al., 2004. *Contrib. Astron. Obs. Skalnaté Pleso* 34, 45.  
 Skopal, A., Vaňko, M., Pribulla, T., Chochol, D., Semkov, E., Wolf, M., Jones, A., 2007. *Astron. Nachr.* 328, 909.